

WHAT DO HYDROGEN ABUNDANCES AT THE MOON'S SOUTH POLE IMPLY FOR ICE PROSPECTING IN SHACKLETON CRATER? R. C. Elphic¹, D. J. Lawrence¹, Vincent R. Eke², Luis F. A. Teodoro³, G. Jeffrey Taylor⁴, D. B. J. Bussey⁵, ¹Space Science and Applications Group, Mail Stop D466, Los Alamos National Laboratory, Los Alamos, NM 87545 USA (relphic@lanl.gov). ²Department of Physics, University of Durham, South Road, Durham DH1 3LE, UK, ³Astronomy and Astrophysics Group, Department of Physics and Astronomy, Kelvin Building, University of Glasgow, Glasgow G12 8QQ, UK, ⁴Hawai'i Institute of Geophysics & Planetology, University of Hawaii, Manoa, HI 96822 USA, ⁵Johns Hopkins Applied Physics Laboratory, Laurel, MD 20723 USA.

Introduction: Permanently shadowed locations at the lunar poles are potential sites for significant concentrations of cold-trapped volatiles, including water ice [1,2]. While results from the Lunar Prospector mission indicate enhanced hydrogen at the poles [3,4,5], some interpret the orbital and Earth-based radar data as indicating the presence of ice [6]; others attribute them simply to rocks and rough topography at small scales [7]. Here we present south pole cold trap water-equivalent hydrogen concentrations that are fully consistent with the orbital neutron measurements. We use a new Pixon-based image reconstruction algorithm together with locations of permanent shadow to effectively improve spatial resolution of Lunar Prospector neutron measurements [8]. We focus on Shackleton Crater, where the inferred crater-average water-equivalent hydrogen (WEH) abundance in permanently shadow is ~0.4 wt%. If the hydrogen/ice distribution in Shackleton is inhomogeneous at kilometer scales and less, then much higher abundances are plausible.

South Pole Shadow Model: Clementine imagery and radar observations now leave little doubt that sizeable areas of the Moon's poles are permanently shadowed. Recent analysis of simple craters less than 20 km in diameter yields estimates of approximately 7500 and 6500 km² in permanent shadow for the north and south poles, respectively [9]. Here we combine that model of simple craters with the south pole radar digital elevation model [10], and calculate the illumination given by the lunar spin axis tilt of 1.5° during south polar summer. Finally, illumination derived from Clementine imagery is used to exclude any spuriously shadowed pixels. Our estimated locations of permanent shadow include the floors of Shackleton, Shoemaker, de Gerlache, Faustini and other craters. A total shadowed area of 12,000 km² is obtained for the south polar region.

Pixon Deconvolution Procedure: The LPNS footprint for epithermal neutrons has a FWHM of ~45 km from 30-km altitude. We attempt to deconvolve the mapped epithermal fluxes in order to improve the spatial resolution of the inferred WEH. We initially assemble the ~7 months of low-altitude (30 km) LPNS data in small spatial bins (5 km). We deconvolve the

smoothed map using a variant of the Pixon image restoration technique [8]. This approach sharpens and restores imagery only where it is statistically permissible to do so. The code searches for the least complicated (lowest information content) map that is consistent with the data, the statistical uncertainties and the instrument point-spread function.

We apply a further very powerful constraint to the pixon deconvolution process: locations that are occasionally in sunlight are only permitted to have at most solar wind abundances (≤ 166 ppm H, or 0.15 wt% WEH). Locations in permanent shadow are allowed to have between 0 and 20 wt% WEH. The latter limit is consistent with pore-filled ice in the regolith.

Figure 1, panel A shows the Pixon recovered epithermal count rate map for the region within approximately 5 degrees of the south pole. Panel B shows the corresponding WEH abundance for the same region.

Ice Prospecting in Shackleton: The inferred WEH abundance in south polar permanently shadowed cold traps is inhomogeneous – values range from less than 0.1 to over 1 wt%. This inhomogeneity may well extend to smaller scales within craters as well. In Shackleton we see on average an epithermal count rate consistent with ~0.4 wt% WEH, which could be a linear combination of drier and wetter parcels combined. Panel C shows this trade-off as a color contour plot of the fractional area of 'wet' parcels on the crater floor: the abscissa is $\log_{10}(\text{WEH}_2)$, the assumed water-equivalent hydrogen abundance in 'wet' parcels, while the ordinate is WEH_1 , the water-equivalent hydrogen abundance of 'dry' parcels. The color code denotes the 'wet' area fraction.

We might expect the 'dry' regolith in cold permanent shadow to preferentially retain higher concentrations of solar wind hydrogen than at lower latitudes, owing to lower diffusion rates. Suppose this cold regolith can retain 0.25 wt% WEH from solar wind implantation (about five times the average amount in returned soils and regolith breccias). Then panel C tells us that the 'wet' parcels of ~2 wt% WEH would occupy a fractional area of 0.3; or 'wet' parcels with ~10 wt% WEH would occupy about 0.1 fractional area of the crater floor.

What this means for “water ice” detection from a landed lunar polar mission is shown in panel D. Here we see the number of sites that must be sampled to ensure a 90% probability of detection of “wet” parcels with WEH_2 , given surrounding “dry” parcels with WEH_1 . If the “wet” and “dry” parcels are thought to have 1 wt% and 0.2 wt% WEH respectively, then only 4 or so sites are required. But if “wet” parcels have 20 wt% WEH, then between 15 and 20 sites must be visited to be 90% certain of detection. Thus, thorough sampling over a wide region is necessary to characterize the distribution of WEH. This seems easier to accomplish with a rover that can sample at a broad range of scales than with a point-by-point hopper approach.

References: [1] Watson, K., Murray, B. C. & Brown, H., (1961) *J. Geophys. Res.* **66**, 3033-3045. [2] Arnold, J. R. (1979) *J. Geophys. Res.* **84**, 5659-5668. [3] Feldman W. C. et al. (1998) *Science*, **281**, 1496–1500. [4] Feldman W. C. et al. (2001) *JGR-Planets*, **106**, 23,231-23,251. [5] Lawrence, D. J. et al. (2006) *JGR-Planets*, 111,10.1029/2005JE002637. [6] Nozette S. et al. (1996) *Science*, **274**, 1495-1498. [7] Campbell, D. B. et al. (2006) *Nature* **443**, 835-837. [8] Eke, V. (2001) *Mon. Not. R. Astron. Soc.* **324** (1), 108-118 [9] Bussey, D. B. J. et al. (2003) *GRL*, **30**, doi:10.1029/2002GL016180. [10] Margot, J-L. et al (1999) *Science* **284**, 1658-1660

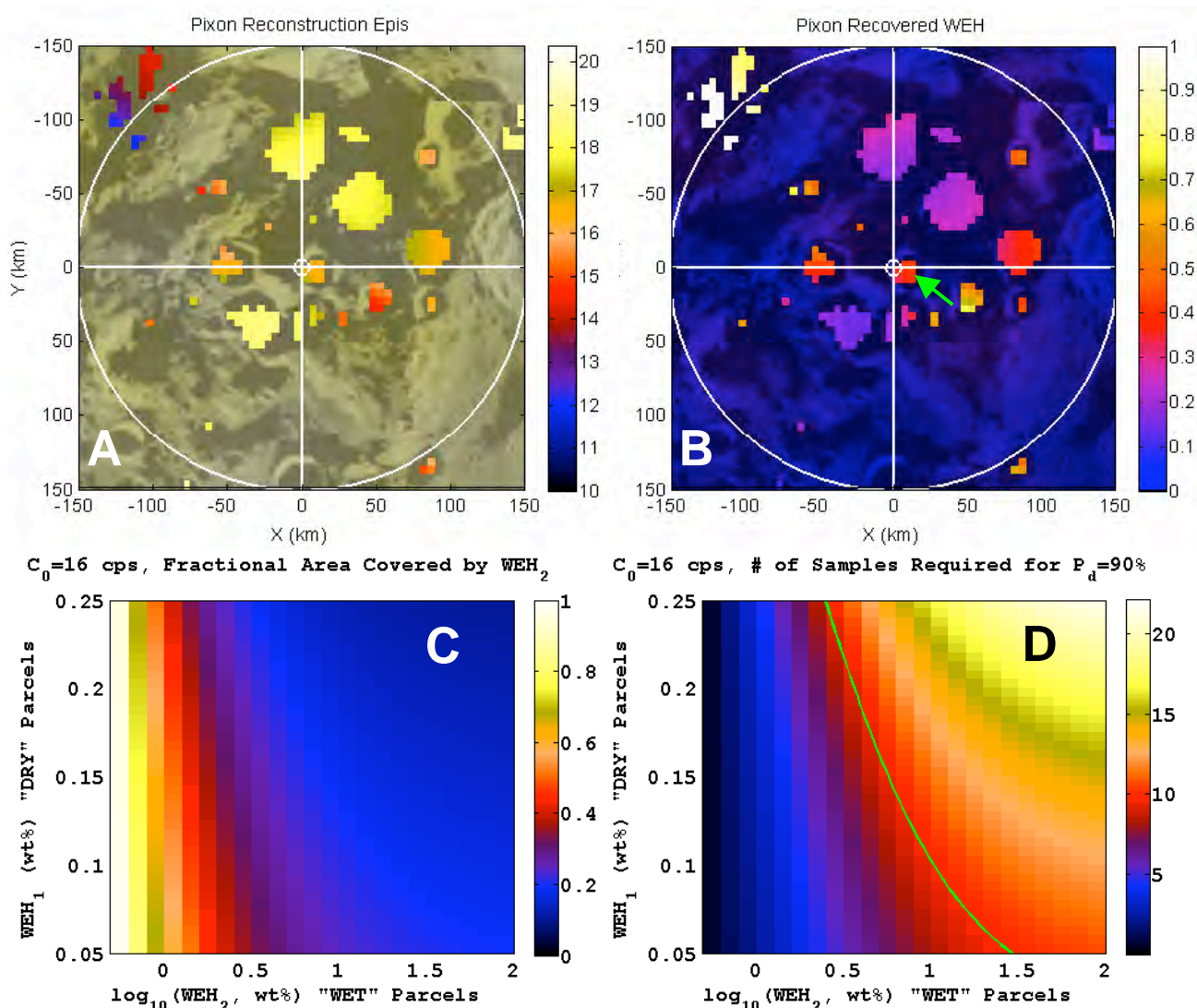


Figure 1. (A) Recovered, deconvolved epithermal count rate map. (B) WEH in wt% from Panel A. Green arrow points to Shackleton crater. (C) Fractional crater floor area covered by ‘wet’ parcels of water-equivalent hydrogen abundance WEH_2 given “dry” parcel WEH_1 . (D) Number of randomly-selected sites needed to provide 90% probability of detection for WEH_2 given “dry” parcel WEH_1 . Green line denotes 10-site contour.